Theor Chem Acc (2002) 108:157–167
DOI 10.1007/s00214-002-0373-7

Theoretical
Chemistry Accounts

Regular article

Internal rotation in squaramide and related compounds. A theoretical ab initio study

Pere M. Deyà, Antonio Frontera, Guillem A. Suñer, David Quiñonero, Carolina Garau, Antoni Costa, Pau Ballester

Departament de Química, Universitat de les Illes Balears, 07071 Palma de Mallorca, Spain

Received: 13 March 2002 / Accepted: 23 June 2002 / Published online: 21 August 2002

Abstract. The structural and energetic changes associated with C–N bond rotation in a squaric acid derivative as well as in formamide, 3-aminoacrolein and vinylamine have been studied theoretically using ab initio molecular orbital methods. Geometry optimizations at the MP2(full)/6-31 + G* level confirmed an increase in the C–N bond length and a smaller decrease in the C = O length on going from the equilibrium geometry to the twisted transition state. Other geometrical changes are also discussed. Energies calculated at the QCISD(T)/6-311 + G** level, including zero-point-energy correction, show barrier heights decreasing in the order formamide, squaric acid derivative, 3-aminoacrolein and vinylamine. The origin of the barriers were examined using the atoms-in-molecules approach of Bader and the natural bond orbital population analysis. The calculations agree with Pauling's resonance model, and the main contributing factor of the barrier is assigned to the loss of conjugation on rotating the C–N bond. Finally, molecular interaction potential calculations were used to study the changes in the nucleophilicity of N and O (carbonyl) atoms upon C–N rotation, and to obtain a picture of the abilities of the molecules to act in non-bonded interactions, in particular hydrogen bonds. The molecular interaction potential results confirm the suitability of squaramide units for acting as binding units in host–guest chemistry.

Key words: Squaric acid amides – Ab initio calculations – Rotational barriers – Molecular interaction potential – Natural bonding orbital theory

1 Introduction

Squaric acid **1** (3,4-dihydroxy-3-cyclobutene-1,2-dione) (Fig. 1) and its derivatives have attracted considerable attention since the parent compound was first reported in 1959 [1, 2]. From the synthetic point of view, **1** is a very powerful C_4-synthon [3] for preparing highly substituted aromatic compounds [4]. It is readily converted to a wide variety of 3,4-disubstituted cyclobutenediones, 4-hydroxycyclobutenones [5] and furanones [3]. While some members of the squaric acid family are key components of advanced materials [6], others have attracted considerable biological interest [7] owing to the well-known ability of squaric acid derivatives to act as stable enolate and carboxylate mimics [8] and their potential as bioisosteric replacements [9].

Recently, we reported the synthesis of several tripodal receptors based on squaramido rings and their application to the recognition of polyalkylammonium compounds [10] and choline-containing phospholipids [11]. We have also reported some theoretical background on squaramide. First, the study of the electronic change of the binding unit owing to hydrogen bonding [12]. Second, the investigation of the physical nature of the interaction by means of calculating the corresponding molecular potential and analyzing the interactional complementarity [13].

Here, we report a theoretical ab initio study on the model compound, 3-hydroxy-4-amino-3-cyclobutene-1,2-dione **2**, a mixed (–OH, $–NH_2$) derivative of **1** and focus our attention on the nature of the C–N bond and its rotational barrier, on the hybridization of the N atom and on its capability as a hydrogen-bond acceptor in binding processes. These are important factors in determining the binding properties of the previously mentioned binding units. Calculations on other model compounds (formamide **3**, 3-aminoacrolein **4** and vinylamine **5**) having different kinds of C–N bonds were also performed for comparison purposes.

Two structural trends are common to all the molecules presented here. First, all the molecules have a conjugated C–N single bond with presumably partial double-bond character in the ground state (resonance model). This double-bond character will be completely lost at the transition state for the C–N bond rotation. Second, the possibility of inversion of the N atom can

Correspondence to: A. Frontera
e-mail: tonif@soller.uib.es

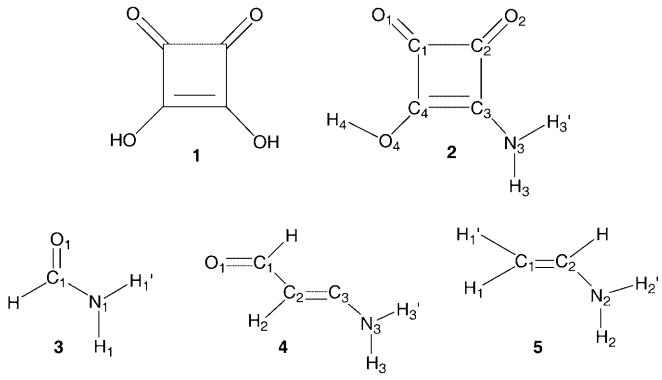

Fig. 1. Squaric acid and atomic numbering for squaramide, formamide, 3-aminoacrolein and vinylamine

lead to a new conformational transition structure. Both the C–N rotation and the N inversion accompany some degree of change in hybridization from the ground state (a mixture of sp^2 and sp^3 character) to sp^3 and sp^2 character at the C–N rotation and N inversion transition states, respectively. Therefore, the changes in the N atom hybridization will be a point of interest in this study.

The resonance model in amides has been questioned by Wiberg and coworkers [14, 15, 16] on the basis of the changes that occur during the rotation of the amido group. The geometrical changes, electron population and electrostatic potentials calculated in the rotation have been used to propose that the O atom does not participate to a significant extent in the rotational barrier. The charge distribution obtained by Bader's method [17] on all the molecules investigated, **2**, **3**, **4** and **5**, agrees with Wiberg's proposal (Fig. 1). However, we will evince that the resonance model is appropriate to describe the amide bond by means of the atomic charges computed using the natural bond orbital (NBO) method, the molecular interaction potential (MIP) and ^{17}O NMR chemical shifts.

2 Computational methods

Geometry optimizations and frequency calculations were performed with GAUSSIAN 94 [18] at the MP2(full)/6-31 + G* level of theory, which leads to quite good geometrical parameters [19]. Diffuse functions were included in order to treat the lone pairs properly [20]. To obtain more satisfactory energies, calculations were carried out at the QCISD(T)/6-311 + G**//MP2(full)/6-31 + G* level. Vibrational frequencies and the corresponding zero-point energies (ZPE) were calculated at the MP2(full)/6-31 + G* level.

The analysis of the electronic wave functions was carried out by using both NBO [21] population analysis and the topological theory of atoms-in-molecules (AIM) [17] as implemented in GAUSSIAN 94 [22, 23] and the PROAIM package [24]. The charge distribution and the atomic properties presented here are derived from the MP2(full)/6-311 + G**//MP2(full)/6-31 + G* calculations.

MIP calculations were carried out by means of the MOPETE [25] program in order to analyze the effect of C–N bond rotation and changes in the N substitution pattern on the hydrogen-bond-acceptor character of the N and O (carbonyl) atoms.

Finally, absolute NMR shieldings were calculated using the gauge including atomic orbital method [26] at the MP2/6-311 + G**//MP2(full)/6-31 + G* level. ^{17}O NMR chemical shifts of **2**–**5** were determined by comparison with the ^{17}O NMR isotropic shifts computed for water (single molecule) at the same level.

3 Energies and structures

Four stationary points (Fig. 2) were initially located and characterized [27] on the corresponding potential hypersurface: the ground state **2**, the 90° and 270° rotamers (**TS2** and **TS1** respectively) and a totally planar geometry initially assigned to the transition state for the N inversion **TSi** (see later). Frequency analysis was performed to verify the ground-state or transition-state character of all the structures presented here. The ZPEs derived from these calculations were scaled by a factor of 0.9661. Actually this factor corresponds to the MP2(full)/6-31G(d) method but the magnitude of this value should not differ appreciably from that for the method used here, MP2(full)/6-31 + G*. Relevant geometric parameters for the aforementioned structures are reported in Table 1.

Selected structural parameters for several stationary states along the rotational path, of **3**, **4** and **5** are shown in Fig. 3. The computed equilibrium structures presented here are in good agreement with previously reported theoretical [28, 29] and experimental [30] values.

Several geometrical parameters for the squaramide ground state are noteworthy. First, the remarkably long C_1–C_2 bond distance that we found in **2** and its rotamers, which is comparable to X-ray structural data of related compounds [31] and can be explained by hyperconjugative interactions between the carbonyl O lone pairs and the adjacent σ^* C_1–C_2 molecular orbital. Second, the NH_2 group in **2** is not coplanar with the four-membered ring, suggesting that the N atom does not have exact sp^2 hybridization as would be expected for the N in an amide group. For comparison purposes, we mention that calculations on formamide carried out by Wiberg et al. [32] at the MP2/6-311 + + G** level found a nonplanar structure with the amine hydrogens about 15° out of plane. Its energy differs by only 2 cal/mol from that of the planar structure, too small to be significant at any practical theoretical level. In our case the difference in energy between **2** and **TSi** is higher

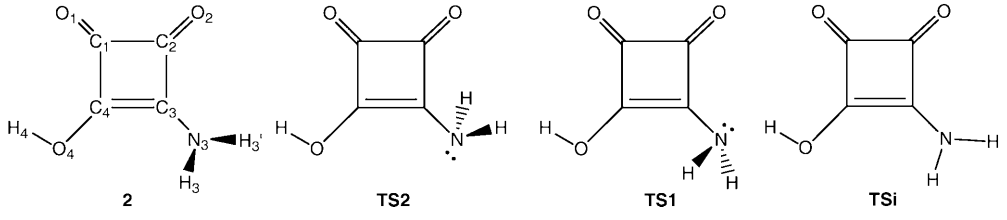

Fig. 2. Stationary points located on the potential surface of **2**

(0.5 kcal/mol) but smaller than the zero-point vibrational energy corresponding to the amino wagging mode of **2** (386 $cm^{-1} = 0.6$ kcal/mol). Third, the NH_2 triangle is bent toward the O (carbonyl) atom, in agreement with the results reported for formamide [28].

From the calculated energies reported in Table 2, several general considerations can be drawn. First, the relative energy values, E_{rel}, show that the barriers calculated at the MP2 level are somewhat larger than those at the self-consistent-field level, in agreement with reported results [33]. The inclusion of highly correlated treatments such as CCSD [33] or QCISD (this work) together with a perturbative correction for the effects of triple excitations [CCSD(T) or QCISD(T)] leads to a significant lowering in the barriers. The addition of the ZPE correction decreases the energy barrier, in agreement with previously reported high-level calculations [28, 33]. The calculated barrier heights were considerably lower than the experimental ones measured in various solvents [34, 35, 36, 37]. As discussed in the literature [38, 39], one possible explanation for this disagreement is the intermolecular interaction with the solvent, since either proton-donating solvents [38] or solvents with a high dielectric constant [39] increase the rotational barrier height.

It can be observed that the rotational barriers decrease in the following order: formamide, squaramide, 3-aminoacrolein and, finally, vinylamine. Consequently, at first sight, this order agrees with what one would expect by considering the relative importance of the respective zwiterionic "amide-type resonance" structure analogous to **3a** (Fig. 4).

Table 1. Selected structural parameters [MP2(full)/6–31 + G*] of the squaramide C–N rotamers shown in Fig. 2

Parameter	Structure				Variation Δ(TS2–2)
	Squaramide	TS2	TS1	TSi	
Bond lengths (Å)					
C_1–C_2	1.544	1.557	1.561	1.544	0.012
$C_1 = O_1$	1.223	1.218	1.218	1.224	−0.005
$C_2 = O_2$	1.221	1.218	1.214	1.222	−0.004
C_3–N_3	1.342	1.405	1.405	1.337	0.063
C_4–O_4	1.339	1.326	1.331	1.340	−0.013
C_1–C_4	1.473	1.493	1.492	1.471	0.021
C_2–C_3	1.488	1.492	1.495	1.489	0.004
$C_3 = C_4$	1.387	1.378	1.379	1.387	−0.008
N_3–H_3	1.013	1.022	1.020	1.012	0.009
N_3–$H_{3'}$	1.014	1.022	1.020	1.013	0.008
Angles (degrees)					
C_3–N_3–H_3	120.5	110.2	111.5	122.2	−10.3
C_3–N_3–$H_{3'}$	117.9	110.2	111.5	119.5	−7.7
C_4–O_4–H_4	108.4	108.7	108.8	108.4	0.2
Dihedral angles (degrees)					
H_3–N_3–C_3–$H_{3'}$[a]	154.4	117.3	120.5	180.0	−37.2
C_3–C_4–O_4–H_4	178.3	180.0	180.0	179.5	1.8

[a] H_3–N_3–C_3–$H_{3'}$ values stand for the dihedral angle formed by the H_3–N_3–C_3 and the H_3–N_3–$C_{3'}$ planes. The corresponding value for a "pure" sp^2 hybridization would be 180°, and 120° for sp^3

4 Discussion

4.1 Geometries

When comparing the changes in the structural parameters for **2** on going to the saddle point rotamers **TS2** and **TS1** (Table 1) with those corresponding to **3**, **4** and **5** (Fig. 3), the following observations can be made. The C–N bond in **2** is lengthened by 0.063 Å, a smaller increment than the corresponding one for **3** (0.080 Å, Fig. 3) but larger than for **4** and **5** (0.061 and 0.038 Å, respectively). In addition, the $C_1 = O_1$ bond is more affected by the rotation than $C_2 = O_2$ in **2**, comparable to **4** and less than in **3** (Table 1, Fig. 3). The shortening of

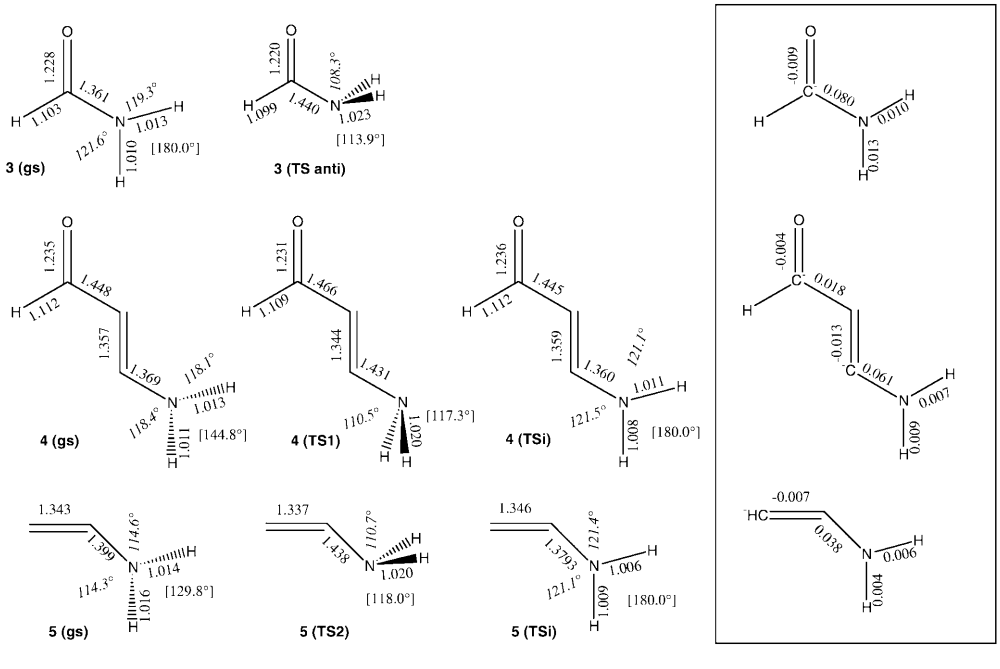

Fig. 3. Selected structural parameters [MP2(full)/6–31G*] for stationary points of systems **3**, **4** and **5**. Distances in angstroms, angles (in *italic*) and dihedral angles [in *parentheses*] in degrees. Bond length differences on passing from the ground state (*gs*) to the C–N rotation transition state (*TS*) are shown in the *box* on the *right*

Table 2. Calculated energies. Total energies are given in hartrees, relative energies and zero-point energies (*ZPE*) are given in kilocalories per mole. GS, TS1, TS2 and TSi represent ground state, 90°, 270° C–N rotamers and the NH_2 inversion transition state, respectively

Computed	HF/6-31G**		MP2(full)/6-31 + G*		QCISD(T)[a]		ZPE[b]	$\Delta\Delta H$	Observed
	E	E_{rel}	*E*	E_{rel}	*E*	E_{rel}			
Formamide									
GS	–		−169.42 1868	0.0	−169.53 9560	0.0	28.51	0.0	
TS anti	–		−169.39 4249	17.3	−169.51 5792	14.9	28.37	14.8	17–22[c]
Squaramide									
GS	−432.21 5194	0.0	−433.45 9693	0.0	−433.70 1528	0.0	45.01	0.00	
TS1	−432.19 7977	10.8	−433.43 6683	14.4	−433.62 8798	11.8	44.28	11.0	
TS2	−432.20 0704	9.1	−433.43 9761	12.5	−433.68 5712	9.9	44.35	9.3	16–18[d]
TSi	–		−433.45 9402	0.2	−433.70 0782	0.5	44.12	–[e]	
3-Aminoacrolein									
GS	−245.81 2859	0.0	−246.55 5702	0.0	−246.73 0420	0.0	50.22	0.0	
TS1	−245.79 7735	9.5	−246.53 8526	10.8	−246.71 6424	8.8	49.62	8.2	
TS2	−245.79 6232	10.4	−246.53 6543	12.0	−246.71 4237	10.2	49.68	9.6	
TSi	−245.81 2643	0.1	−246.55 5297	0.3	−246.72 9166	0.8	49.67	0.2	
Vinylamine									
GS	−133.07 5154	0.0	−133.50 4310	0.0	−133.62 8588	0.0	43.88	0.0	
TS1	−133.06 4970	6.4	−133.49 3042	7.1	−133.61 8227	6.5	43.48	6.1	
TS2	−133.06 7034	5.1	−133.49 5415	5.6	−133.62 0817	4.9	43.50	4.5	6.7[f]
TSi	–	–	−133.50 1954	1.5	−133.62 5030	2.2	43.01	1.3	1.0–1.3[g]

[a] QCISD(T) = QCISD(T)/6-311 + G**//MP2(full)/6-31 + G*
[b] The MP2(full)/6-31 + G* ZPEs were scaled by 0.9661. See Ref. [27]
[c] Ref. [35]
[d] This value is approximate since it corresponds to 3-diethylamino-4-ethoxycyclobutenedione [36]. The barrier for the NH_2 derivative will be lower by several kilocalories per mole
[e] Ref. [32]
[f] The calculated rotational barrier is somewhat lower than the experimental estimation of 6.7 kcal/mol [37]
[g] See Ref. [30]

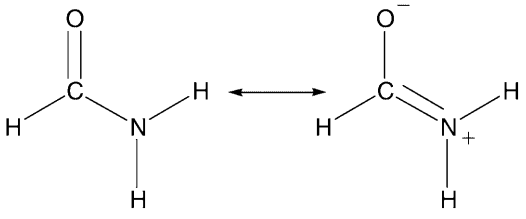

Fig. 4. Zwiterionic amide-type resonance structure of formamide

the $C_1 = O_1$ and $C_3 = C_4$ bonds and the lengthening of the C_1–C_4 bond on rotation of the C–N bond are in agreement with the loss of conjugation of the N atom lone pair through the cyclobutenedione system, which will exclude **TS2a** as a resonance form (Fig. 5). Another important change occurs for the C_4–O_4 bond length, which decreases by 0.013 Å on going from **2** to the **TS2** rotamer, thus suggesting a slight increase in double-bond character and supporting the idea that the resonance form **TS2b** increases its contribution to the composite. The latter observations highlight that C_3 and the N_3 atoms are involved in the most important geometric changes during C–N rotation, in accordance with Wiberg's model.

The degree of pyramidalization of the N atom, represented by the H_3–N_3–C_3–$H_{3'}$ dihedral angle (Table 1, Fig. 3), decreases in the following order: formamide, squaramide, 3-aminoacrolein and, finally, vinylamine. There is a good linear correlation between the dihedral angle values and the calculated rotational barrier, suggesting that the most important factor is the change in hybridization (partially sp^2 to practically sp^3) on rotation.[1] The value of the slope is small but positive (0.2), which supports Wiberg's [14, 15, 16] hypothesis that an important factor contributing to the rotational barrier is the need for the N to stabilize its lone pair.

4.2 Atomic properties

In order to explore the C–O and C–N bonds features of the compounds studied here, the charge density variations caused on rotating the amino group were initially examined from the point of view of Bader's theory [17] (Table 3). Integration of the charge density showed a net change of 0.030*e* for the O carbonyl of the squaramide and 3-aminoacrolein, being about half of what was found for formamide (0.055*e*). These values are in agreement with the known [40] attenuation of electronic effects along the chain caused by the two carbon CH = CH fragments between the C = O and the NH_2 groups in **2** and **4**, suggesting poor involvement of the O atom in the vinylogous amide resonance.[2]

[1] The correlation coefficient, r^2, of the linear plot is 0.9925, being the sum of squares error equal to 0.4038

[2] It is a classical example of the use of the reaction constant, ρ, of the Hammett equation to measure the efficiency of various groups in transmitting electronic effects. The attenuation factor assigned to the CH = CH group is 0.48, in good agreement with the relationship between the charge shifts found for the carbonyl O in **2** or **4** (0.030*e*) and **3** (0.055*e*)

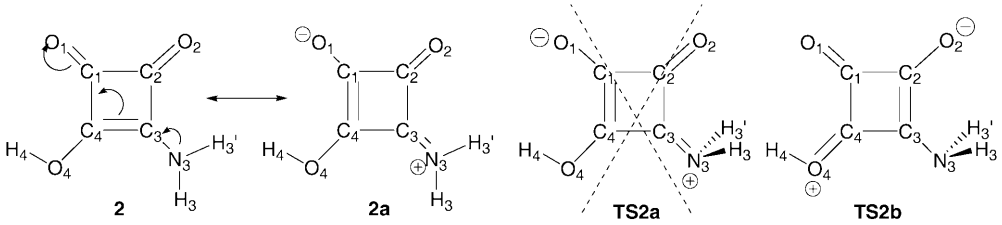

Fig. 5. Loss of conjugation of the N atom lone pair through the cyclobutenedione system, which will exclude **TS2a** as a resonance form

The electronic changes at the C–N bond upon rotation are more complex: in **3**, C_1 increases its electron density by 0.151*e*, whereas in the vinylogous derivatives **2** and **4**, the C_3 atom increases its electron density by 0.101*e* and 0.113*e*, respectively. The C_1, C_2 and C_4 electron densities remain practically unchanged. The changes in the electron density of the N atoms are more significant, going from 0.157*e* in **3** to 0.144*e*, 0.122*e* and 0.066*e* in **2**, **4** and **5**, respectively. AIM charges show that the magnitude of the changes are significantly lower when the NH_2 group charges are used instead of the N atomic charges. In the AIM theory the charges assigned to two bonded atoms are strongly dependent on the location of the boundary (determined by the zero-flux surface) between them. This location is affected by the difference in the electronegativity between the two atoms. In fact, the change in the electronegativity of the N atom in passing from the ground state to the transition state produces a variation in the location of the boundary between the N atom and the three atoms directly bonded to it (C and the two H atoms); therefore, part of the depletion of the N charge density is directed towards the two H atoms. Consequently, the observed $N \rightarrow C$ charge-density transfer would be better described by the charge shifts corresponding to the NH_2 group and the C atom.

In order to test charge shifts upon rotation from another point of view, we carried out a NBO population analysis. It is well known that the NBO analysis, as well as other methods based on atomic orbitals that are assigned to specific atoms [41, 42], gives different results than Bader's treatment [15]. In formamide, the main differences concern the C (carbonyl) and N atomic charges for which NBO and AIM analyses give opposite results (Table 3). Whereas changes in the NBO population of formamide point toward an O to N flow of charge on C–N rotation, AIM analysis proposes that the carbonyl carbon gains electronic population at the expense of the amide N [14]. One general trend can be envisaged. Regardless of the method used, the O atom (carbonyl) loses charge density upon rotation, with the most relevant charge shifts corresponding to the NBO analysis for all the compounds calculated.

For example, in **4** most of the AIM charge shifts involve the N and the C_3 atoms, with the O atom being affected to a minor extent. NBO charges also show changes in the C–N bond, although the major change is located on the C_2 atom. A clear difference between both methods is the charge shift of the N atom, which is negative (−0.052*e*) for NBO and positive for AIM (0.122*e*). This difference is also observed in the other molecules calculated.

NBO charge analysis of **2** shows a change in the $C_1 = O_1$ and C_3–NH_2 groups. Another remarkable change is that concerning the O_4–C_4 bond where the impossibility of the NH_2 group to donate charge to the ring when rotated is compensated with the electron donation from O_4. This fact help us to understand the electronic behavior of the squaramide ring on C–N rotation.

The flow of electronic population between the atoms may be envisaged, according to AIM theory, by considering the relative changes in atomic electronegativities caused by the differences in the N hybridization during C–N bond rotation. In the ground-state conformers, the hybridization at N would be close to sp^2, whereas on going to the transition states the amino group undergoes pyramidalization, showing a close sp^3 hybridization. The lowering in *s* character explains that the N atom would be much less electronegative in the transition conformers than in the ground state, thus diminishing the withdrawing effect over the rest of the molecule and being the origin of a new distribution of electronic population in which the rest of the atoms of the molecule become smoothly more stabilized. This explanation takes into account mainly the σ-electron system. On the other hand, NBO population analysis concludes that the impossibility of C to N π overlap in the rotated form prevents the electronic flow from N to C atoms, thus increasing the atomic charge of the N on going from the ground state to the rotated transition state. In conclusion, it is possible to obtain a more realistic picture of the electronic flow considering the so-called σ–π polarization phenomenon [42] that includes both aforementioned explanations.

In summary, the differences between the NBO and AIM analyses carried out for **2**, **3** and **4** are mainly located on the computed charges at N and O atoms. Apart from the most important difference, i.e. the opposite sign of the charge shift of the N atom upon rotation, the magnitude of the charge shifts are also significant. The AIM analysis always predicts charge shifts much greater at the N atom than at the O atom. This fact together with the small carbonyl bond length decrease compared to the C–N bond length increase upon rotation support Wiberg's model. The NBO analysis predicts similar charge shifts at N and O atoms, thus behaving as in π-conjugated systems.

4.3 Bond properties

The properties of the charge density at the (3,−1) bond critical points (CP) may be useful to discuss the changes caused by C–N bond rotation (Table 4). By focusing our

Table 3. Atoms-in-molecules (*AIM*) and natural bond orbital (*NBO*) charges, group charges and charge shifts [TS-GS] upon C–N bond rotation. [MP2(full)/6–311 + G**//MP2 (full)/6–31 + G*]. See Fig. 1 for the atomic labels. *TS* stands for the C–N rotation process transition state

Atom	GS		TS		Charge shifts	
	AIM	NBO	AIM	NBO	AIM	NBO
Squaramide						
O_1	−1.091	−0.655	−1.061	−0.609	0.030	0.046
C_1	1.001	0.519	0.995	0.530	−0.006	0.011
O_2	−1.079	−0.631	−1.077	−0.626	0.002	0.005
C_2	1.007	0.554	1.000	0.548	0.007	−0.006
C_4	0.535	0.258	0.556	0.348	0.021	0.090
C_3	0.488	0.162	0.387	0.088	−0.101	−0.074
N_3	−1.210	−0.819	−1.066	−0.851	0.144	−0.032
O_4	−1.130	−0.711	−1.118	−0.687	0.012	0.024
NH_2	−0.343	−0.001	−0.292	−0.095	0.051	−0.094
OH	−0.520	−0.207	−0.508	−0.185	0.012	0.022
C_1O_1	−0.090	−0.136	−0.054	−0.079	0.036	0.057
Formamide						
O	−1.120	−0.710	−1.065	−0.620	0.055	0.090
C	1.475	0.690	1.324	0.695	−0.151	0.005
N	−1.224	−0.875	−1.067	−0.929	0.157	−0.054
H	0.027	0.099	0.056	0.107	0.029	0.008
NH_2	−0.382	−0.080	−0.315	−0.182	0.067	−0.102
CH	1.502	0.789	1.380	0.812	−0.122	0.023
CO	0.355	−0.020	0.259	0.075	−0.096	0.095
3-Aminoacrolein						
O	−1.071	−0.665	−1.041	−0.625	0.030	0.040
C_1	0.958	0.512	0.959	0.506	0.001	−0.006
H	−0.007	0.089	0.010	0.102	0.017	0.013
C_2	−0.055	−0.456	−0.040	−0.351	0.015	0.105
C_3	0.446	0.198	0.333	0.144	−0.113	−0.054
N	−1.179	−0.832	−1.057	−0.884	0.122	−0.052
NH_2	−0.366	−0.060	−0.329	−0.149	0.037	−0.089
CO	−0.113	−0.153	−0.082	−0.119	0.031	0.034
Vinylamine						
C	−0.070	−0.498	−0.048	−0.363	0.022	0.135
C	0.379	0.093	0.318	0.023	−0.061	−0.070
N	−1.127	−0.849	−1.061	−0.873	0.066	−0.024
NH_2	−0.377	−0.121	−0.356	−0.172	0.021	−0.051

attention on the C–N bond CP we can see that the magnitude of the charge density decreases by one-tenth when the corresponding interatomic distance lengthens. The moderate change in this magnitude is similar in all the compounds, and can be attributed to a little loss of covalent bonding between C and N. The increase in $\rho(r)$ found for the C_4–O_4 bond, accompanied by a slight augmentation of the ellipticity indicates the π character of the O_4-ring interaction. The Laplacian of the charge density ($\nabla^2\rho$) at the C–N bond CP upon rotation remains essentially unchanged. For **2** and **3** the $\nabla^2\rho$ at the C = O bond CP changes its sign upon rotation, indicating a discrete increase in the polar character of the bond. In the C–N bond the bonded radius of the C atom increases in all cases, while that of the N atom decreases slightly. Consequently, the lengthening of the C–N bond is mainly due to the increase in the size of the C atom, indicating a net gain of charge density from the neighboring N. The rest of the bond CP properties are relatively insensitive to the C–N rotation [15].

As already stated, the AIM results presented here and the analyses derived from them support Wiberg's amide bond model in which the C = O bond, particularly the O atom, does not participate (is a spectator) in the rotation of the C–N bond. However, the NBO method predicts the opposite trend. To solve this dilemma, we extended our study in order to know which model, i.e. the resonance or Wiberg's model, is appropriate for a true definition of the controversial amide bond.

4.4 Molecular interaction potential

MIP calculations have been shown to be valuable tools for exploring molecular reactivity [43] but also to rationalize and predict molecular interactions [44]. Since the MIP is based on the molecular electrostatic potential (MEP) with further addition of a classical repulsion–dispersion term, MIP is able to represent not only electrostatic interactions but also steric effects. For these reasons, MIP will be used to describe nonbonded interactions, in particular hydrogen bonds.

In order to better describe the suitability of the compounds tested in this study to serve as hydrogen-bond acceptors, in particular **2** and **3**, we carried out MIP calculations starting from ab initio MP2(full)/6–311 + G** wave functions. MIPs were computed for the interaction with a positive classical particle (charge 0.5) having van der Waals characteristics of a hydrogen bound to an electronegative atom [MIP (1/2 H^+)], thus simulating a hydrogen bond. The results are shown in Fig. 6 and Table 5.

Table 4. Bond critical point properties and bond orders. All values are in atomic units except r_a and r_b, which are in angstroms. The properties of the charge density are calculated at bond critical points. $\rho(r)$ is the charge density, $\nabla^2\rho(r)$ the Laplacian of the charge density, ε the ellipticity of the bond, r_a and r_b the bonded radii. Atomic labels correspond to the ones shown in Fig. 1. The covalent bond orders were calculated by means of the methodology implemented in Gaussian 94 by Cioslowski and Mixon [22]

Bond	$\rho(r)$	$\nabla^2\rho(r)$	ε	Bond order	r_a	r_b
Squaramide GS						
C_1–C_2	0.243	−0.531	0.115	–[a]	0.773	0.775
C_1=O_1	0.390	−0.022	0.061	–	0.415	0.808
C_2=O_2	0.391	−0.015	0.062	–	0.415	0.807
C_1–C_4	0.272	−0.663	0.182	–	0.703	0.772
C_2–C_3	0.265	−0.629	0.136	–	0.712	0.778
C_3=C_4	0.311	−0.837	0.284	–	0.696	0.695
C_3–N_3	0.321	−0.800	0.062	–	0.477	0.865
C_4–O_4	0.295	−0.225	0.004	–	0.448	0.892
N_3–H_3	0.331	−1.672	0.052	–	0.755	0.237
N_3–$H_{3'}$	0.330	−1.684	0.052	–	0.758	0.236
Squaramide TS2						
C_1–C_2	0.238	−0.513	0.088	0.925	0.790	0.770
C_1=O_1	0.393	0.050	0.053	1.415	0.412	0.806
C_2=O_2	0.394	0.032	0.055	1.407	0.413	0.805
C_1–C_4	0.265	−0.640	0.127	0.989	0.719	0.778
C_2–C_3	0.265	−0.621	0.163	1.051	0.735	0.759
C_3=C_4	0.319	−0.878	0.327	1.457	0.662	0.719
C_3–N_3	0.296	−0.898	0.065	1.024	0.565	0.841
C_4–O_4	0.304	−0.202	0.059	0.934	0.442	0.884
N_3–H_3	0.326	−1.517	0.046	0.815	0.753	0.249
N_3–$H_{3'}$	0.326	−1.517	0.046	0.815	0.753	0.249
Formamide GS						
H–C	0.278	−0.970	0.029	0.901	0.372	0.716
C=O	0.392	−0.168	0.090	1.333	0.418	0.811
C–N	0.312	−0.808	0.096	1.045	0.483	0.877
N–H_1	0.333	−1.661	0.056	0.788	0.750	0.239
N–$H_{1'}$	0.331	−1.669	0.053	0.800	0.754	0.238
Formamide TS anti						
H–C	0.282	−0.997	0.029	0.912	0.364	0.720
C=O	0.395	0.051	0.102	1.417	0.411	0.808
C–N	0.285	−0.840	0.049	0.945	0.592	0.849
N–H_1	0.324	−1.476	0.041	0.824	0.751	0.253
N–$H_{1'}$	0.324	−1.476	0.041	0.824	0.751	0.253
3-Aminoacrolein GS						
H–C_1	0.271	−0.915	0.019	0.919	0.381	0.716
C_1=O	0.381	−0.066	0.068	1.406	0.418	0.818
C_1–C_2	0.284	−0.764	0.157	1.092	0.724	0.724
C_2=C_3	0.325	−0.930	0.347	1.630	0.632	0.725
C_3–N_3	0.306	−0.799	0.054	1.071	0.488	0.881
N_3–H_3	0.334	−1.651	0.055	0.804	0.751	0.242
N_3–$H_{3'}$	0.333	−1.637	0.052	0.806	0.750	0.240
3-Aminoacrolein TS1						
H–C_1	0.274	−0.933	0.018	0.921	0.377	0.718
C^1=O	0.384	−0.018	0.069	1.429	0.415	0.816
C_1–C_2	0.278	−0.749	0.105	1.040	0.735	0.731
C_2=C_3	0.338	−1.000	0.360	1.702	0.657	0.687
C_3–N_3	0.283	−0.833	0.043	0.998	0.573	0.858
N_3–H_3	0.328	−1.493	0.048	0.838	0.748	0.254
N_3–$H_{3'}$	0.328	−1.493	0.048	0.838	0.748	0.254
Vinylamine GS						
C_1–C_2	0.331	−0.949	0.418	1.782	0.634	0.709
C_2–N_2	0.292	−0.838	0.060	1.027	0.517	0.884
N_2–H_2	0.332	−1.566	0.050	0.829	0.748	0.247
N_2–$H_{2'}$	0.333	−1.574	0.054	0.830	0.747	0.247
Vinylamine TS2						
C_1–C_2	0.340	−1.006	0.412	1.794	0.657	0.680
C_2–N_2	0.277	−0.804	0.027	0.988	0.570	0.868
N_2–H_2	0.329	−1.487	0.049	0.849	0.746	0.254
N_2–$H_{2'}$	0.329	−1.487	0.049	0.849	0.746	0.254

[a]Unfortunately the bond order calculation, as well other AIM atomic properties, corresponding to the GS squaramide **2** was impossible to carry out by the aforementioned implementation since the program stops with an error message; therefore, the corresponding bond order values are not available

MIP maps of **3** were computed in the carbonyl plane, since it is the most informative concerning the hydrogen-bond formation. Initial inspection of the maps clearly shows that in the planar form, the O region is the only suitable hydrogen-bond acceptor. The value of the MIP minimum originating from the interaction with the lone pairs is −17.4 kcal/mol. Computation of the MIP along the line perpendicular to the molecular plane passing through the N atom, reveals a minimum energy located at 2.1 Å having an energy of only −1.19 kcal/mol, in agreement with the poor nucleophilic character of the amide N atom and reflecting the π conjugation.

The most important differences between the MIP energy maps computed at the ground and the transition states are located in the N area, where a significant minimum on the molecular plane is found in the rotated form (−13.9 kcal/mol). The energy depth (in absolute value) of the MIP minimum close to the O atom slightly decreases on rotating the C–N bond (−14.9 kcal/mol), indicating a lower nucleophilicity. In summary, the O atom in the equilibrium geometry is a better nucleophile than in the rotated form, whereas the N atom becomes a good nucleophile in the twisted conformer. These results are in agreement with those previously reported by Luque and Orozco [45] from MEP calculations and by Wiberg and coworkers [14] from two pertinent quantities readily obtained from the wavefunctions: the Laplacian of the charge density calculated on the molecular van der Waals surface [17, 46] and the electrostatic potential [47]. It must be mentioned that the results are in accord with the predictions of the resonance model.

The MIP maps for **4** are parallel to those of **3** (Fig. 6). In the two conformers, we found the lowest minimum in the molecular plane and close to the carbonyl O atom, deeper in the planar (−18.0 kcal/mol) than in the rotated form (−14.9 kcal/mol). A second region of the MIP minimum is located near the expected position of the N atom lone pair (−14.9 kcal/mol) in the 90°-twisted conformer.

The squaramide MIP map is a little more complex (Fig. 6). The ground state of **2** shows several minima near the area presumably occupied by the lone pairs of the two carbonyl O atoms, the lowest minimum being located in the vicinity of O_1 (−16.3 kcal/mol). The region between the two carbonyl O atoms has a considerable energy depth ranging from −12.0 to −13.0 kcal/mol, thus indicating a large area suitable for accepting hydrogen bonds. The "out-of-plane" MIP in the O_4 region shows two energy minima, above and below the molecular plane (at 2.3 Å from the O atom), of −1.0 and −0.6 kcal/mol, respectively.

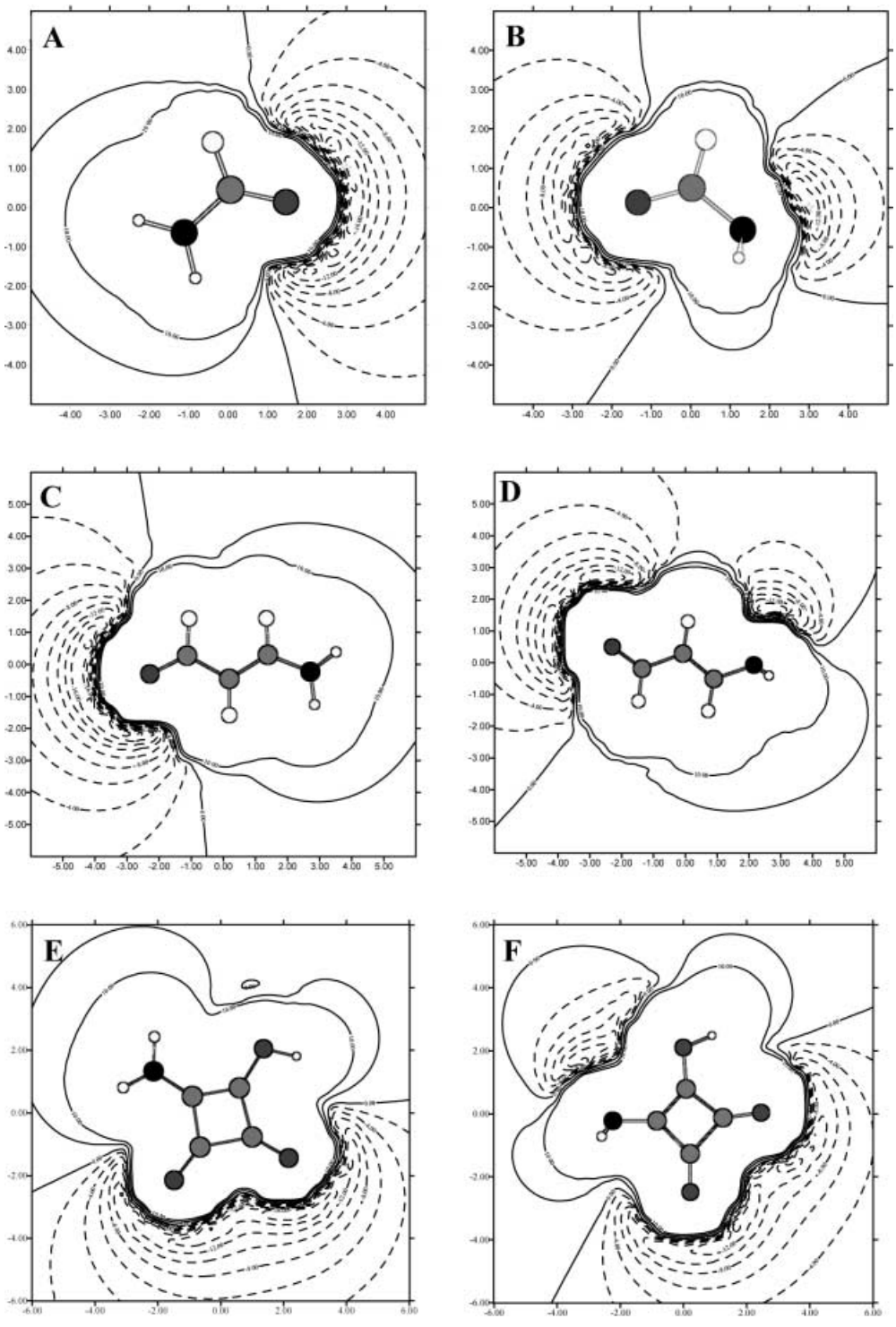

Fig. 6. MP2(full)/6–311 + G** molecular interaction potential maps calculated in the molecular plane corresponding to the ground state and transition state for **a**, **b** formamide, **c**, **d** 3-aminoacrolein and **e**, **f** squaramide, respectively. The isopotential lines are in kilocalories per mole and the coordinates are in angstroms. Negative and positive isopotential lines are represented by *dashed* and *solid* lines, respectively. The orientation of the structures corresponds to the standard coordinates of the Gaussian calculation

The latter has a smaller energy depth owing to the nuclear repulsion term corresponding to the hydrogen atoms of the amino group. Another local minimum of only −0.3 kcal/mol is found 2.1 Å above the N atom in a direction perpendicular to the molecular plane. Again, it agrees with the poor nucleophilicity of the N atom, presumably involved in the ring conjugation.

When the squaramide C–N bond rotates, a second region of the MIP minimum appears in the vicinity of the N atom, with an interaction potential of −11.2 kcal/mol. Similarly, there are some changes in the MIP topology around the two carbonyl area, in such a way that the lowest minimum is actually found near O_2 (−1-3.9 kcal/mol), thus reinforcing the aforementioned argument that O_4 donates charge density to the ring when the C–N bond rotates.

All these observations suggest, in agreement with Pauling's resonance model, that when the C–N bond is rotated, the nucleophilicity of the carbonyl O atom decreases. Accordingly, the MIP results suggest that the

Table 5. ^{17}O NMR chemical shifts (ppm) relative to water and molecular interaction potential (*MIP*) depth values (kcal/mol)

Compound	GS		TS	
	^{17}O NMR	MIP	^{17}O NMR	MIP
Squaramide	446 (O_1)	−16.3 (C=O_1)	526 (O_1)	−12.8 (C=O_1)
	470 (O_2)	−15.4 (C=O_2)	491 (O_2)	−13.9 (C=O_2)
		−0.3 (NH_2)		−11.2 (NH_2)
Formamide	390	−17.4 (C=O)	602	−14.9 (C=O)
		−1.2 (NH_2)		−13.9 (NH_2)
3-Aminoacrolein	568	−18.0 (C=O)	630	−14.9 (C=O)
		−5.1 (NH_2)		−14.9 (NH_2)

Table 6. Influence of the N substitution in the disquaramide on the charge and hydrogen-bond-acceptor capabilities of carbonyl O atoms. For CHELPG charges see Ref. [50]. The MIP was calculated at the MP2(full)/6–311+G**//MP2 (full)/6–31+ G* theoretical level

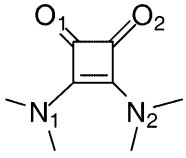

Disquaramide substitution		Atomic charges CHELPG		MIP [1/2 H^+] (kcal/mol)
N_1	N_2	O_1	O_2	
H,H	H,H	−0.444	−0.444	−17.8
Me,H	H,H	−0.447	−0.461	−18.3
Me,H	Me,H	−0.469	−0.469	−18.7
Me,Me	Me,H	−0.452	−0.481	−19.7
Me,Me	Me,Me	−0.490	−0.490	−21.0

electron flow in the equilibrium structures presented here goes from N to C, and part of this charge moves toward to the O. This effect decreases in the following order: **3**, **4** and **2**.

With the aim to assess the applicability of the resonance model to squaramides, additional calculations on disquaramide derivatives having different substitution patterns were carried out in order to evaluate the changes in the hydrogen-bond-acceptor capabilities of the carbonyl O atoms by increasing the substitution at the N. The results (Table 6) clearly support the classical Pauling model since the greater the N atom substitution the deeper is the MIP minimum near the corresponding conjugated carbonyl O and the more negative is its atomic charge.

4.5 ^{17}O NMR calculations

Dahn and coworkers [48, 49] have shown that the chemical shift values in ^{17}O NMR spectra are very clearly different for doubly (=O) and singly (–O–) bonded O atoms and that both, but particularly the former, are very sensitive to electronic influences and resonance effects. The ^{17}O NMR technique is a valuable tool to probe π-bond order or π-electron density around O atoms. The computed ^{17}O NMR chemical shifts of **2**, **3** and **4** are summarized in Table 5. The chemical shift of **3** is 390 ppm, in acceptable agreement, taking into account the deshielding influence of the hydrogen bonds in water, with the experimental value of 304 ppm [49]. The 90°-rotated form of **3** gives a computed chemical shift of 602 ppm, close to the experimental value of acetone (569 ppm). The observed difference in the chemical shift of **3** upon rotation is large (212 ppm), in agreement with the charge shift predicted by the NBO method on the O atom (0.090*e*). For **4** and **2**, the computed chemical shift increments are only 62 and 80 ppm for O_1 and 21 ppm for O_2, respectively. These results are also in agreement with the NBO charge shifts obtained for the O atoms (Table 3). The large difference observed in **3** confirms that the O atom is not an spectator and is an active participant in the C–N rotation. The differences observed for **4** and **2** are considerable, indicating that the O atom is affected by the rotation of the NH_2 group.

5 Conclusions

AIM computational results, including changes upon rotation in electron population and other atomic and bond properties studied here, support Wiberg's amide bond model and show small-to-moderate changes in their corresponding values. The linear correlation found between the degree of hybridization of the computed equilibrium structures and the height of the rotational barrier supports the hypothesis that one important factor is the need for the N atom to stabilize its lone pair electrons as well as possible. The lack of more significant changes in the bond and ring CP makes difficult the study of the squaramido ring electronic structure and the charge density flow.

In contrast, our NBO, MIP and ^{17}O NMR results clearly support the Pauling Scheme and that in the planar geometries the electron flow is in the N → C → O direction, thus increasing the nucleophilicity of the O amidic carbonyl when conjugation is possible. In fact, MIP calculations on several N-methyl-substituted disquaramides reveal an increase in the corresponding conjugated carbonyl O negative charge as well as in the depth of the MIP minimum by augmenting the substitution on the N atoms, thus supporting the applicability of the resonance model and offering a possibility to modulate the hydrogen-bond-acceptor character of the carbonyl O atoms. Additional examples, theoretical calculations as well as additional experimental evidence are necessary to better understand the intimate aspects of the electron flow inside these molecules. Concerning the binding behavior of the squaramido unit, it shows a large region (between the two carbonyl O atoms) of a deep MIP suitable for accepting hydrogen bonds, in contrast with formamide, which shows a slightly more negative MIP minimum confined in a minor binding area. This is important, considering that the larger the area potentially active as a hydrogen-bond acceptor, the greater is the number of hydrogen atoms that can point toward that region at a time. This would be the case for H_4N^+ or $(CH_3)_4N^+$ types of cations, for which the possibility to form several hydrogen-bond interactions with each squaramido unit must favor the binding process. The large potential binding region of the squaramido structures clearly confirms that squaramido-based host molecules [10, 11] are powerful receptors for intervening in molecular recognition processes with adequate positively charged guests.

The results from ab initio calculations clearly indicate a decrease in the C–N bond rotational barrier on going from formamide to squaramide and finally to 3-amino-acrolein. This trend is corroborated by the NBO charge shifts of the O atom and the computed ^{17}O NMR chemical shifts, indicating more π conjugation (charge transfer toward the O atom) in formamide than in either squaramide or 3-aminoacrolein.

Bearing in mind the limitations of any qualitative model, the present results support the validity of the amide resonance model.

Acknowledgements. This investigation was supported by the Dirección General de Investigación Científica y Técnica (project PB98–0129). We thank M. Orozco and F.J. Luque for making their MOPETE-97 program available to us, and S. Olivella for helpful suggestions. A.F. thanks the MEC for a postdoctoral grant. D.Q. and C.G. thank the Universitat de les Illes Balears and the FSE, respectively, for predoctoral fellowships. The calculations were performed at the Centre de Supercomputació de Catalunya and on our own computers at the Universitat de les Illes Balears.

References

1. (a) Cohen S, Lacher JR, Park JD (1959) J Am Chem Soc 81: 3480; (b) Maahs G, Hegenberg P (1966) Angew Chem Int Ed Engl 5: 888
2. (a) Ried W, Schmidt AH (1972) Angew Chem Int Ed Engl 11: 997; (b) Schmidt AH, Ried W (1978) Synthesis 1; (c) Knorr H, Ried W (1978) Synthesis 649; (d) Schmidt AH, Ried W (1978) Synthesis 869; (e) Schmidt AH (1980) Synthesis 961
3. (a) Yamamoto Y, Ohno M, Eguchi S (1994) J Org Chem 59: 4707; (b) Yamamoto Y, Ohno M, Eguchi S (1994) Tetrahedron 26: 7783
4. (a) Moore HW, Perri ST (1988) J Org Chem 53: 996; (b) Foland LD, Karlsson JO, Perri ST, Schwabe R, Xu SL, Patil S, Moore HW (1989) J Am Chem Soc 111: 975; (c) Perri ST, Moore HW (1990) J Am Chem Soc 112: 1897; (d) Xu SL, Taing M, Moore HW (1991) J Org Chem 56: 6104; (e) Xia H, Moore HW (1992) J Org Chem 57: 3765; (f) Krysan DJ, Gurski A, Liebeskind LS (1992) J Am Chem Soc 114: 1412; (g) Liebeskind LS, Wang J (1993) J Org Chem 58: 3550; (h) Gurski A, Liebeskind LS (1993) J Am Chem Soc 115: 6101
5. (a) Reed MW, Pollart DJ, Perri ST, Foland LD, Moore HW (1988) J Org Chem 53: 2477; (b) Liebeskind LS, Fengel RW, Wirtz R, Shawe TT (1988) J Org Chem 53: 2482; (c) Liebeskind LS, Yu MS, Yu RH, Wang J, Hagen KS (1993) J Am Chem Soc 115: 9048; (d) Ohno M, Yamamoto Y, Shirasaki Y, Eguchi S (1993) J Chem Soc Perkin Trans 1 263; (e) Yamamoto Y, Nunokawa K, Ohno M, Eguchi S (1993) Synlett 781
6. (a) Fabian J, Nakazumi H, Matsuoka M (1992) Chem Rev 92: 1197; (b) Law K-Y (1993) Chem Rev 93: 449; (c) Schmidt AH (1980) In: West R (ed) Oxocarbons. Academic, New York, p 185; (d) Diederich F, Rubin Y (1992) Angew Chem Int Ed Engl 31: 1101; (e) Hopf H, Maas G (1992) Angew Chem Int Ed Engl 31: 931; (f) Seitz G, Imming P (1992) Chem Rev 92: 1242; (g) Sun Pu L (1991) J Chem Soc Chem Commun 429
7. (a) Cole RJ, Kirksey JW, Cutler HG, Doupnik BL, Peckham JC (1973) Science 179: 1324; (b) Tietze LF, Arlt M, Beller M, Glüsenkamp KH, Jähde E, Rajewsky MF (1991) Chem Ber 124: 1215; (c) Kinney WA, Lee NE, Garrison DT, Podlesny EJ Jr, Simmonds JT, Bramlett D, Notvest RR, Kowal DM, Tasse RP (1992) J Med Chem 35: 4270
8. (a) Pirrung MC, Han H, Ludwig RT (1994) J Org Chem 59: 2430; (b) Ueda Y, Crast LB Jr, Mikkilineni AB, Partyka RA (1991) Tetrahedron Lett 32: 3767; (c) Kim CU, Misco PF (1992) Tetrahedron Lett 33: 3961; (d) Soll RM, Kinney WA, Primeau J, Garrick L, McCaully RJ, Colatsky T, Oshiro G, Park CH, Hartupee D, White V, McCallum J, Russo A, Dinish J, Wojdan A (193) Bioorg Med Chem Lett 3: 757; (e) Chan PCM, Roon RJ, Koerner JF, Taylor NJ, Honek JF (1995) J Med Chem 38: 4433
9. (a) Thornber CW (1979) Chem Soc Rev 8: 563; (b) Lipinski CA (1986) Annu Rep Med Chem 21: 283
10. (a) Tomàs S, Rotger MC, González JF, Deyà PM, Ballester P, Costa A (1995) Tetrahedron Lett 36: 2523; (b) Tomàs S, Prohens R, Vega M, Rotger MC, Deyà PM, Ballester P, Costa A (1996) J Org Chem 61: 9394; (c) Prohens R, Tomàs S, Morey J, Deyà PM, Ballester P, Costa A (1998) Tetrahedron Lett 39: 1063
11. Tomàs S, Prohens R, Deslongchamps G, Ballester P, Costa A (1999) Angew Chem Int Ed Engl 38: 2208
12. (a) Quiñonero D, Frontera A, Ballester P, Deyà PM (2000) Tetrahedron Lett 41: 2001; (b) Quiñonero D, Frontera A, Deyà PM (1999) 5th World Congress of Theoretically Oriented Chemists, Imperial College, London. Book of Abstracts. p 395
13. (a) Quiñonero D, Frontera A, Tomàs S, Suñer GA, Morey J, Costa A, Ballester P, Deyà PM (2000) Theor Chem Acc 104: 50; (b) Quiñonero D, Frontera A, Suñer GA, Morey J, Costa A, Ballester P, Deyà PM (2000) Chem Phys Lett 326: 247; (c) Quiñonero D, Garau C, Frontera A, Ballester P, Costa A, Deyà PM (2002) Chem Eur J 8: 433; (d) Quiñonero D, Prohens R, Garau C, Frontera A, Ballester P, Costa A, Deyà PM (2002) Chem Phys Lett 351: 115
14. (a) Wiberg KB, Breneman CM (1992) J Am Chem Soc 114: 831; (b) Wiberg KB, Laidig KE (1987) J Am Chem Soc 109: 5935
15. Wiberg KB, Rablen PR (1995) J Am Chem Soc 117: 2201
16. Wiberg KB, Hadad CM, Breneman CM, Laidig KE, Murcko MA, LePage TJ (1991) Science 252: 1266
17. Bader RFW (1990) Atoms in molecules: a quantum theory. Oxford University Press, Oxford

18. Frisch MJ, Trucks GW, Schlegel HB, Gill PMW, Johnson BG, Robb MA, Cheeseman JR, Keith T, Petersson GA, Montgomery JA, Raghavachari K, Al-Laham MA, Zakrzewski VG, Ortiz JV, Foresman JB, Cioslowski J, Stefanov BB, Nanayakkara A, Challacombe M, Peng CY, Ayala PY, Chen W, Wong MW, Andres JL, Replogle ES, Gomperts R, Martin RL, Fox DJ, Binkley JS, Defrees DJ, Baker J, Stewart JP, Head-Gordon M, Gonzalez C, Pople JA (1995) GAUSSIAN 94, revision D2. Gaussian, Pittsburgh, Pa
19. Hehre WJ, Radom L, Schleyer PvR, Pople JA (1986) Ab initio molecular orbital theory. Wiley, New York
20. Clark T, Chandrasekhar J, Spitznagel GW, Schleyer PvR (1983) J Comput Chem 4: 294
21. Glendening ED, Reed AE, Carpenter JE, Weinhold F. NBO version 31. Department of Chemistry, University of Winsconsin, Madison
22. Cioslowski J, Mixon ST (1991) J Am Chem Soc 113: 4142
23. (a) Cioslowski J, Surjan PR (1992) J Mol Struct 255: 9; (b) Cioslowski J (1992) Chem Phys Lett 194: 73; (c) Cioslowski J, Nanayakkara A, Challacombe M (1993) Chem Phys Lett 203: 137; (d) Cioslowski J (1994) Chem Phys Lett 219: 151
24. (a) Biegler-König FW, Bader RFW, Tang T-H (1982) J Comput Chem 3: 317; (b) Bader RFW, Tang T-H, Tal Y, Biegler-König FW (1982) J Am Chem Soc 104: 946.
25. Luque FJ, Orozco M (1997) MOPETE-97 program. Universitat de Barcelona
26. Wolinski K, Hinto JF, Pulay P (1990) J Am Chem Soc 112: 8251
27. Scott AP, Radom L (1996) J Phys Chem 100: 16502
28. (a) Fogarasi G, Szalay PG (1997) J Phys Chem A 101: 1400
29. (a) Oie T, Topol IA, Burt SK (1995) J Phys Chem 99: 905; (b) Ou M-C, Chu S-Y (1995) J Phys Chem 99: 556; (c) Wiberg KB, Rablen PR (1995) J Am Chem Soc 117: 2201; (d) Laidig KE, Cameron LM (1993) Can J Chem 71: 872; (e) Kieninger M, Suhai S (1996) J Mol Struct 375: 181; (f) Laidig KE, Cameron LM (1996) J Am Chem Soc 118: 1737
30. (a) Kitano M, Kuchitsu K (1974) Bull Chem Soc Jpn 47: 67; (b) Blom CE, Grassi G, Bauder A (1984) J Am Chem Soc 106: 7427; (c) Brown RD, Gogfrey PD, Kleibomer B, Pierlot AP, McNaughton D (1990) J Mol Spectrosc 142: 195
31. (a) Rathna A, Chandrasekhar J (1991) J Chem Soc Perkin Trans 2 1661; (b) LePage T, Nakasuji K, Breslow R (1985) Tetrahedron Lett 26: 5919; (c) Semmingsen D, Hollander FJ, Koetzle TF (1977) J Chem Phys 66: 4405; (d) Cerioni G, Janoschek R, Rappoport Z, Tidwell TT (1996) J Org Chem 61: 6212
32. Wiberg KB, Hadad CM, Rablen PR, Cioslowski J (1992) J Am Chem Soc 114: 8644
33. Burton NA, Chiu SS-L, Davidson MM, Green DVS, Hillier IH, McDouall JJW, Vincent MA (1993) J Chem Soc Faraday Trans 89: 2631
34. Taha AN, Neugebauer Crawford SM, True NS (1998) J Am Chem Soc 120: 1934
35. Drakenberg T (1972) Tetrahedron Lett 13: 1743
36. Thorpe JE (1968) J Chem Soc B 435
37. Hamada Y, Sato N, Tsuboi M (1987) J Mol Spectrosc 124: 172
38. (a) Jasien PG, Stevens WJ, Krauss M (1986) J Mol Struct (THEOCHEM) 139: 197; (b) Neuman RC Jr, Woolfenden WR, Jonas V (1969) J Phys Chem 73: 3177; (c) Drakenberg T, Dahlqvist K-I, Forsen S (1972) J Phys Chem 76: 2178
39. Duben AJ, Miertus S (1982) Chem Phys Lett 88: 395
40. (a) Jones RAY (1987) Physical and mechanistic organic chemistry, 2nd edn. Cambridge University Press, Cambridge, p 42; (b) Perrin DD, Dempsey B, Serjeant EP (1981) pK_a prediction for organic acids and bases. Chapman and Hall, London; (c) Page M, Williams A (1997) Organic & bio-organic mechanisms. Addison Wesley Longman, Reading, Mass, p 259
41. (a) Reed AE, Weinstock RB, Weinhold F (1985) J Chem Phys 83: 735; (b) Gobbi A, Frenking G (1993) J Am Chem Soc 115: 2362
42. Reed AE, Curtiss LA, Weinhold F (1988) Chem Rev 88: 899
43. Orozco M, Luque FJ (1993) J Comput Chem 14: 587
44. Hernández B, Orozco M, Luque FJ (1997) J Comput-Aided Mol Des 11: 153
45. Luque FJ, Orozco M (1993) J Chem Soc Perkin Trans 2: 683
46. Carroll MT, Chang C, Bader RFW (1988) Mol Phys 63: 387
47. Scrocco E, Tomasi J (1978) Adv Quantum Chem 11: 115
48. Dahn H, Ung-Truong M-N (1987) Helv Chim Acta 70: 2130
49. Christ HA, Diehl P, Schneider HR, Dahn H (1961) Helv Chim Acta 44: 865
50. Breneman CM, Wiberg KB (1990) J Comput Chem 11: 361